



 Cite this: *RSC Adv.*, 2021, 11, 6791

# Structures and impact strength variation of chemically crosslinked high-density polyethylene: effect of crosslinking density

 Yueqing Ren, \* Xiaojie Sun, Lanlan Chen, Yafei Li, Miaomiao Sun, Xuelei Duan and Wenbin Liang

Impact strength of high-density polyethylene (HDPE), especially at low temperature, is crucial for its applications outdoors because of its poor impact strength. In order to improve the impact strength of HDPE, crosslinked HDPE was prepared by the addition of a peroxide crosslink agent, bis(*tert*-butyldioxyisopropyl)benzenehexane, and the effect of the crosslinking density on the microstructures and mechanical properties, especially impact strength between  $-60\text{ }^{\circ}\text{C}$  and  $23\text{ }^{\circ}\text{C}$ , were investigated. The results show that the crosslinking density is controlled by varying the content of the crosslinking agent. It is found that, at room temperature, with increase in the content of crosslink agent from 0% to 0.5–0.7%, the impact strength increases from  $4\text{ kJ m}^{-2}$  to about  $80\text{ kJ m}^{-2}$  and the elongation at break increases from 20% to about 550%. With further increase in the content of crosslink agent to 1.5%, the impact strength and the elongation at break reduce to  $64\text{ kJ m}^{-2}$  and 360% respectively. With increase in crosslink agent, the flexural modulus, yield strength, crystallinity, mean lamellar thickness, crystal size and spherulitic size and the brittle–ductile transition temperature (BDTT) decrease, and the gel content, impact strength of the HDPE at low temperature, intensity of  $\beta$  transition increase significantly. In considering both the room temperature mechanical properties and low temperature impact strength, the optimized content of the crosslink agent is about 0.7%. Overall, crosslinking significantly improves the toughness and impact strength of HDPE and extends its application, especially at low temperature.

 Received 9th December 2020  
 Accepted 30th January 2021

DOI: 10.1039/d0ra10365a

[rsc.li/rsc-advances](http://rsc.li/rsc-advances)

## 1. Introduction

Polyethylene (PE) is one of the most popular plastics in many sectors of industry because of its relative good processability, chemical resistance and low cost.<sup>1,2</sup> Compared with low-density polyethylene (LDPE) and linear low-density polyethylene (LLDPE), high-density polyethylene (HDPE) has relatively lower content of short and long chain branching, and higher melting temperature and modulus. However, the usefulness of HDPE as an engineering thermoplastic is still limited due to its poor impact resistance, especially under extreme conditions such as punctured at low temperature. The challenge of improving toughness continues to attract considerable interest.<sup>3–7</sup>

HDPE toughened by melt blending has attracted much attention as a simple and cost-effective method.<sup>7</sup> The toughening of HDPE with elastomers is a well-known method due to its high toughening efficiency and easy operation for industrial scale production. The toughening efficiency of elastomers is related to the volume fraction, rubber particle size and molecular parameters, *e.g.* molecular weight, glass transition temperature, *etc.* HDPE toughened by elastomers with lower

glass transition temperature ( $T_g$ ) has generally higher impact strength and lower brittle–ductile transition temperature (BDTT).<sup>5</sup> Besides melt mixing with elastomer, toughening of HDPE with a rigid filler is also a commonly practiced method.<sup>4,6,8–11</sup> The stiffness, strength and toughness of HDPE/filler system increase simultaneously although the toughness efficiency is inferior to HDPE/elastomer system. While in contrast, the stiffness and strength of elastomer-toughened HDPE often decrease significantly with increase in elastomer content. Moreover, the dispersion of elastomer or/and filler in the polymer matrix is usually poor due to the incompatible nature and poor interfacial adhesion between polymer matrix and toughness modifier, resulting in poor mechanical properties.<sup>12</sup>

Crosslinking is one promising method for the modification of the polyethylene.<sup>13–16</sup> A crosslinking reaction of polyethylene can be carried out in three ways: a chemical crosslinking reaction by organic peroxide, high-energy radiation crosslinking and silence-water crosslinking.<sup>17</sup> The final result of crosslinking processing is introduction of crosslink or bridge between the macromolecular chains and forms a crosslinked network. The crosslinked network has great effects on the crystallization process through its influence on mobility and nucleation of molecular chains, which is related to the mechanical properties

National Institute of Clean-and-Low-Carbon Energy, Future Science City, Changping District, Beijing 102211, China. E-mail: yueqing.ren@chnenergy.com.cn



of semicrystalline polymers.<sup>18–24</sup> Smedberg discovered that PE with high molecular weight, high content of vinyl groups and low number of long chain branches had higher crosslinkability, network quality and thermal stability after crosslinked by peroxide.<sup>25,26</sup> Khonakdar found that stress at break, modulus, yield strength, elongation at break and  $T_g$  generally decreased with increase in crosslink density for the crosslinked PE because of decrease in crystallization and increase in molecular mobility and free volume.<sup>14,27</sup> Wang of our lab investigated the effect of stretching temperature on the puncture resistance of peroxide crosslinked polyethylene films and found that the puncture resistances of the films stretched above melting temperature ( $T_m$ ) were much larger than that stretched below  $T_m$ .<sup>28</sup> Generally speaking, the molecular mobility, free volume and  $T_g$  of polymer are related to its impact strength, especial impact strength at different temperature. However, studies of the effect of crosslinking on PE were mainly focused on crystallization characteristics, tensile properties, creep properties, electrical properties, and the mostly on LDPE and LLDPE. In this article, a chemical crosslinking reaction by a peroxide crosslink agent, bis(*tert*-butyldioxyisopropyl)benzene-hexane (BIPB), is used. BIPB is a lower odor crosslink agent in comparison with dicumyl peroxide. The effect of the crosslinking content on the impact strength of HDPE, especially at different temperature, is investigated. Investigation of structure evolution of the crosslinked HDPE has been carried out by differential scanning calorimetry (DSC), wide angle X-ray diffraction (WAXD), polarized light microscopy (PLM), dynamic mechanical analysis (DMA) and scanning electron microscopy (SEM). The relationships between microstructures and impact properties are also discussed.

## 2. Experimental

### 2.1 Materials

A commercial grade high density polyethylene grade HDPE2911 was purchased from Fushun Petrochemical Company, China. The melt flow index is 26 g/10 min and the density is 0.960 g cm<sup>-3</sup>. Bis(*tert*-butyldioxyisopropyl)benzenehexane (BIPB, grade Luperox® F flakes) was used as the peroxide crosslink agent and supplied by Arkema Chemical Co, Ltd. Tris(2,4-di-*tert*-butylphenyl) phosphite grade Irgafos® 168 was used as antioxidant and purchased from BASF. All the materials were used as received without further treatments.

### 2.2 Samples preparation

The HDPE and other additives were blended by a Haake PTW16 co-rating twin-screw extruder. The content of antioxidant was fixed at 0.1 wt% in order to inhibit possible thermal degradation during mixing. The content of crosslink agent varied from 0 to 1.5 wt%. The mixing process was carried out at 140 °C at the screw speed of 100 rpm. At this state, the crosslink agent BIPB mixed with HDPE and other additives without going through crosslinking reaction because the mixing temperature was not sufficient to activate the peroxide initiation reaction.

Sample for rheological characterization was prepared by hot press molded using a Platen press P 300 (Collin, Germany) laboratory hot press at 140 °C. The pressure was 100 bar, maintained for 3 min and then cooled to ambient temperature with a cooling rate of 10 °C min<sup>-1</sup>.

Crosslinked sample for mechanical properties and structural characterization was prepared by hot press at 200 °C and pressure of 100 bar for 5 min, during which the crosslinking took place. Then the sheet was cooled to ambient temperature with a cooling rate of 10 °C min<sup>-1</sup>. The thickness of the crosslinked sheet was about 4 mm. The crosslinked sample was maintained for 24 h for further characterization.

### 2.3 Measurement

**2.3.1 Gel content.** Gel content was determined by xylene extraction according to the ASTM D2765 standard. Approximately 0.3 g of sample was placed in a pouch made by 120 mesh stainless steel cloth and extracted in boiling xylene for 12 h to remove the soluble part of PE. After extraction, the samples were dried to a constant mass at 150 °C. The gel content was calculated according to the following equation:

$$\text{Gel content} = \frac{m_1}{m_0} \times 100\%$$

where  $m_1$  is the final mass after extraction and  $m_0$  is the initial mass of the sample.

**2.3.2 Rheological behavior.** Rheological behavior was measured by a Discovery Hybrid HR-2 rheometer (TA instruments) under nitrogen. A temperature sweep model was used to determine the change of complex viscosity,  $\eta^*$ , during the crosslinking process. A parallel plate configuration with a diameter of 25 mm and a gap of 1 mm was used for all tests. The temperature increased from 140 °C to 200 °C at a heating rate of 10 °C min<sup>-1</sup> and then maintained for 10 min. The strain was 1% and the frequency was 1 Hz.

**2.3.3 Differential scanning calorimetry (DSC).** Crystallization characteristics were investigated by a Q2000 differential scanning calorimetry (DSC). About 5 mg of the sample were measured under nitrogen atmosphere in a heat-cool method. The sample was heated from 0 to 180 °C, held for 5 min, and then cooled to 0 °C. The heating rate and cooling rate were 10 °C min<sup>-1</sup>. The crystallinity ( $X_{c,dsc}$ ) was calculated by using the following equation:

$$X_{c,dsc} = \frac{\Delta H_m}{\Delta H_{100\%}} \times 100$$

where  $\Delta H_m$  is the integrated melting enthalpy of the melting peak between 0 °C and 150 °C from DSC endothermic curve,  $\Delta H_{100\%}$  is the melting enthalpy of polyethylene crystal with 100% crystallinity in this study.<sup>29</sup> The mean lamellar crystal thickness ( $l_{dsc}$ ) was calculated using the empirical Gibbs-Thomson equation as follows:

$$l_{dsc} = \frac{2\sigma_e}{\Delta H_f} \frac{T_m^0}{T_m^0 - T_m}$$

where  $T_m$  and  $T_m^0$  are experimental and theoretical melting temperature (K) of polyethylene, respectively, and  $\sigma_e$  is the



lamellar surface free energy,  $\Delta H_f$  is the melting enthalpy of the lamella with infinite thickness. The constant parameters for polyethylene are  $T_m^0 = 414.5 \text{ K}$ ,  $\sigma_e = 0.07 \text{ J m}^{-2}$  and  $\Delta H_f = 288 \times 106 \text{ J m}^{-3}$ .<sup>29–32</sup>

**2.3.4 Wide-angle X-ray diffraction (WAXD).** The WAXD measurements of the crosslinked HDPE were conducted in a D8 ADVANCE diffractometer, with Cu K $\alpha$  radiation ( $\lambda = 1.5418 \text{ \AA}$ ) at 40 kV and 40 mA. The scanning angles were from  $10^\circ$  to  $90^\circ$ , the scanning step is  $0.02^\circ$  and the scanning frequency is 0.1 s per step. The diffraction patterns data were used to calculate the degrees of crystallinity and the crystallite sizes. Subsequently, the peaks in WAXD were mathematical deconvoluted by using Gaussian function and the overall crystallinity ( $X_{c,xrd}$ ) was calculated by the following equation:

$$X_{c,xrd} = \frac{A_c}{A_c + A_a} \times 100$$

where  $A_c$  and  $A_a$  are the fitted areas of the crystal and amorphous peaks, respectively.<sup>33,34</sup> The apparent crystalline size ( $l_{hkl}$ ) was determined according to the Scherrer's equation:

$$l_{hkl} = \frac{K\lambda}{\beta \cos \theta}$$

where  $\beta$  is the half-width of the diffraction peak,  $K$  is equal to 0.9,  $\theta$  is the Bragg angle. The values of  $l_{hkl}$  for (110) and (200) were calculated.

**2.3.5 Polarized light microscopy (PLM).** Observation of the spherulitic morphology was carried out with an Olympus BX53 Polarized light microscope. Thin slices of 5 mm in thickness were cut from the crosslinked samples by a by a Leica EM UC7 ultramicrotome. The slices were mounted between a glass slide and a cover slip. The magnification ratio was chosen as  $200\times$ .

**2.3.6 Dynamic mechanical analysis (DMA).** Dynamical mechanical properties were investigated using a DMA Q800 apparatus from TA Instruments. The sample dimension was  $18 \times 5 \times 1 \text{ mm}^3$ . A single cantilever clamping mode was used. DMA tests were carried out from  $-100 \text{ }^\circ\text{C}$  to  $50 \text{ }^\circ\text{C}$  with a heating rate of  $3 \text{ }^\circ\text{C min}^{-1}$ . The dynamic strain was 0.1% and the frequency was 10 Hz.

**2.3.7 Impact strength.** Notched Izod impact test at different temperature was performed according to ASTM D256 using a CEAST 9050 impact tester (Instron GmbH) with a thermal chamber. The temperature inside the chamber was lowered using a temperature controller connected to a liquid N<sub>2</sub> supply. The temperature varied from  $-60 \text{ }^\circ\text{C}$  to  $23 \text{ }^\circ\text{C}$ . A V-shaped notch (2 mm) was made at the center of the impact specimen ( $100 \times 10 \times 4 \text{ mm}$ ) by a motorized notching machine (CEAST) with a notch-tip radius of 0.25 mm. The results were averaged over five replicates of each composition.

**2.3.8 Mechanical properties.** Mechanical properties were investigated using an Instron 5965 apparatus according to ASTM D638 standard. The thickness of the sample was 4 mm. The tensile rate was  $50 \text{ mm min}^{-1}$  and the bending rate was  $2 \text{ mm min}^{-1}$ . Each measurement included five samples and the average results were adopted.

## 3. Results and discussions

### 3.1 Rheological properties and gel content

Peroxide crosslinking is a series of free radical reactions induced by high temperature decomposition of peroxide. Active free radical could be generated when peroxide (ROOR') is heated, and then free radical captures hydrogen of PE molecular chain, generating PE molecular chain with free radical. Because PE molecular chain with free radical possesses high reaction activity, crosslinking reaction takes place and inter-molecular chemical bonds generate, when the molecular chain free radicals meet each other (Fig. 1).<sup>35</sup>

To elucidate the effect of crosslinking agent on molecular mobility and network structure, HDPE was crosslinked by different content of BIPB, and the rheological properties and gel content were investigated. The results are shown in Fig. 2 and Table 1. For the peroxide crosslinked polyethylene, the crosslink process is controlled by the temperature of the sample. With increase in the temperature from  $140 \text{ }^\circ\text{C}$  to  $200 \text{ }^\circ\text{C}$ , the peroxide BIPB decomposes and crosslinking processing takes place randomly in the molten state in which the HDPE has only amorphous structure. The complex viscosity remains relatively low below  $170 \text{ }^\circ\text{C}$  (or approximately 150 s). When the temperature reaches above  $175 \text{ }^\circ\text{C}$ , the complex viscosity of the crosslinked HDPE increases rapidly. At about  $200 \text{ }^\circ\text{C}$  (or 350 s.), the complex viscosity reaches the plateau, indicating the completion of the crosslinking process. With increase in BIPB content, the loss factor ( $\tan \delta$ ) decreases, revealing the transition from linear to network structure and, consequently, increase in elasticity. The complex viscosity of the crosslinked HDPE increases significantly with increase in crosslinking temperature as well as crosslinking agent content, and the increased viscosity suggests that the mobility of the molecular chains is prohibited significantly. As shown in Table 1, the gel content increases rapidly with increase in BIPB content in the low concentration region. Above 0.7% BIPB content, the gel fraction gradually increases and appears to become saturated at a maximum gel content of about 96%.

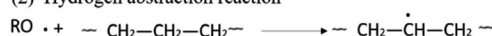
### 3.2 Thermal behaviour

The crystal parameters of semicrystalline polymers have considerable effect on their mechanical properties. The crystallization characteristics were investigated by DSC. The melting curves are shown in Fig. 3 and the crystal parameters

#### (1) Primary radical generation



#### (2) Hydrogen abstraction reaction



#### (3) Recombination of backbone radical



Fig. 1 Diagram of the crosslink reaction.



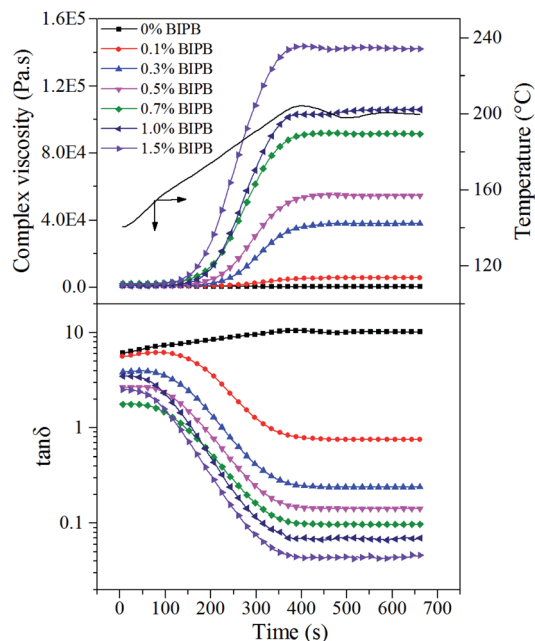


Fig. 2 Rheological properties of the crosslinked HDPE.

Table 1 Gel content of the crosslinked HDPE

BIPB content (%)	Gel content (%)
0	0
0.1	0
0.3	42.5 ± 0.6
0.5	81.3 ± 0.3
0.7	88.1 ± 0.2
1.0	94.0 ± 0.2

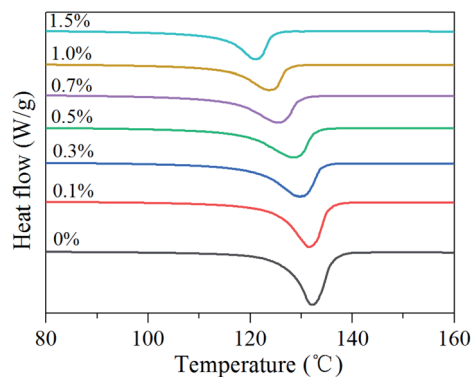


Fig. 3 DSC thermographs of crosslinked HDPE via a heating scan.

are illustrated in Table 2. All the specimens have a distinct melting endothermic peak. With increase in BIPB content, the peak melting temperature ( $T_{mp}$ ) and melting endothermic peak intensity decrease. The crystallinity ( $X_{c,dsc}$ ) decreases from 74.3% to 42.2% and the mean lamellar thickness decreases from 22.0 nm to 10.0 nm. These results indicate that the

Table 2 Crystallization parameters of crosslinked HDPE

BIPB content (%)	$T_{mp}$ (°C)	$X_{c,dsc}$ (%)	$l_{dsc}$ (nm)
0	132.2	74.3	22.0
0.1	131.6	67.1	20.7
0.3	129.8	64.0	17.4
0.5	128	61.1	15.1
0.7	125.5	53.9	12.7
1.0	123.8	44.9	11.5
1.5	121.1	42.2	10.0

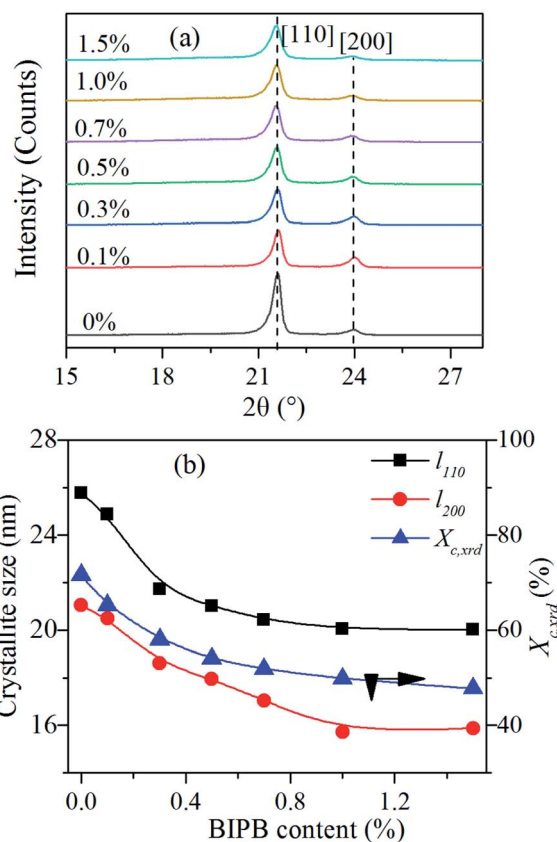


Fig. 4 WAXD diffraction (a) and the crystal parameters (b) of the crosslinked HDPE.

crystallization process and chain folding are prohibited because of the decrease in mobility of the molecular chains after crosslinking by BIPB.

### 3.3 WAXD analysis

The crystal parameters of the crosslinked HDPE were investigated by WAXD. The WAXD data were obtained at room temperature from the crosslinked HDPE samples retaining the thermal history of hot press-molding. The results are shown in Fig. 4. There are two peaks at 21.5° (110) and 23.9° (200) and the position of reflection peaks remains unchanged with increase in BIPB content. On the other hand, as the BIPB content



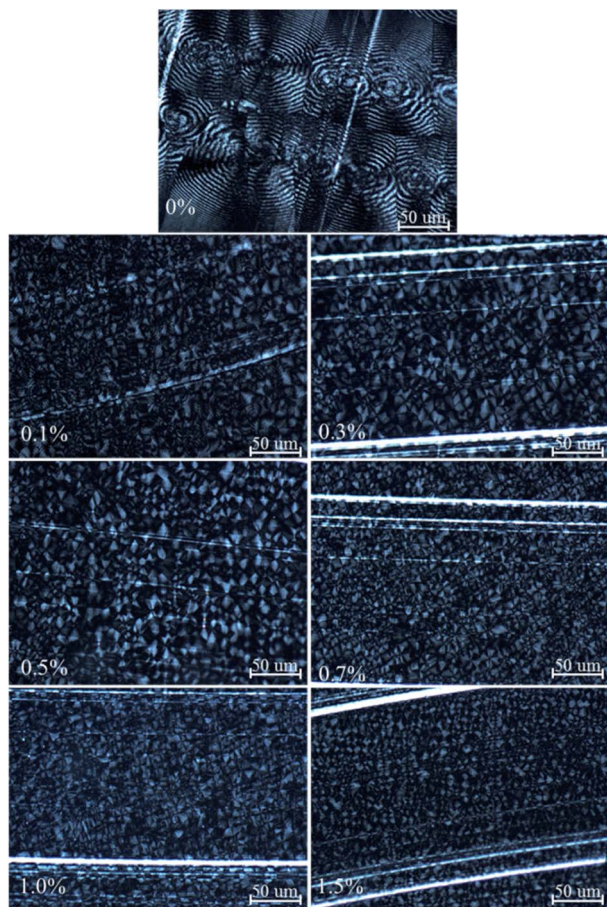


Fig. 5 Polarized optical micrographs of the crosslinked HDPE.

increases, the intensity of the two peaks decreases. Moreover, the crystallinity calculated by XRD data ( $X_{c,xrd}$ ) and the crystallite size of (110) and (200) decrease significantly with initial increase in the content of BIPB. It is interesting to note that, at higher BIPB content, the crystallinity and the crystallite size decrease gradually, with  $l_{110}$  and  $l_{200}$  exhibiting inflecting points at 0.5% and 1.0% BIPB, respectively. The results are consistent with the observed increase in gel content, and prove the strong suppression effects of network on the formation of the crystallite. The WAXD crystallinity data are in good agreement with that of the DSC data.

### 3.4 Polarized light microscopy analysis

The crystal structure of un-crosslinked and crosslinked HDPE was observed using PLM. The results are shown in Fig. 5. With increase in BIPB content, the spherulitic size decreases significantly in the low BIPB content region (below 0.7%) due to the apparent increase in gel content and the suppression of chain folding and growth of spherulites during crystallization. Above 0.7% BIPB, the spherulitic size of the crosslinked HDPE decreases slightly.

For the un-crosslinked and crosslinked HDPE with 0.1% BIPB, the crystal structures exhibit obvious banded spherulites because of the lamellar twist.<sup>36–39</sup> With increase in the content of

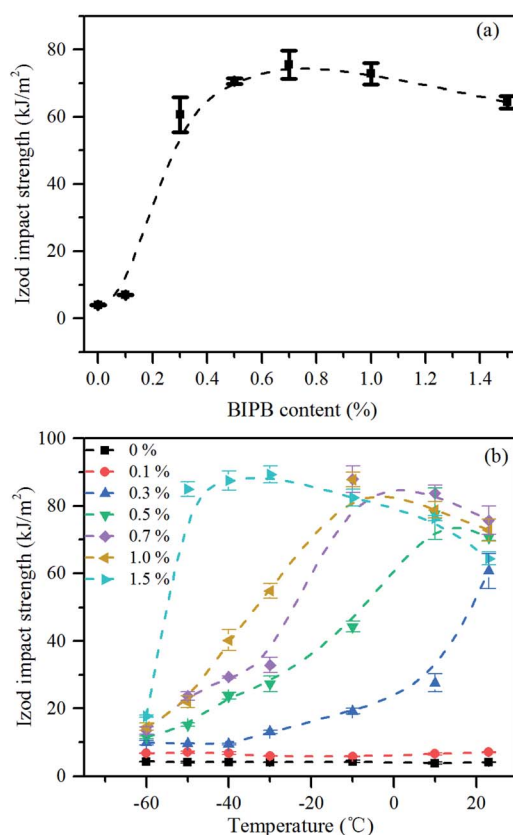


Fig. 6 Impact strength at room temperature, 23 °C, (a) and effect of temperature on the impact strength of crosslinked HDPE (b).

BIPB, the band pattern disappears which is probably due to the suppression of the chain mobility and lamellar twist.

### 3.5 Impact strength

The effect of BIPB content and the testing temperature on the impact strength of crosslinked HDPE were investigated. The results are presented in Fig. 6. As shown in the Fig. 6(a), the impact strength of un-crosslinked and crosslink HDPE with 0.1% BIPB change very little and the impact strength is about 4–6  $\text{kJ m}^{-2}$ . With further increase in BIPB content from 0.1% to 0.7%, the specimen changes from brittle to ductile and the impact strength of the crosslinked HDPE samples increase significantly at room temperature (23 °C) because of the decrease in crystallinity, lamellar thickness<sup>40</sup> and crystallite size<sup>41</sup> and the increase in ductility.<sup>42</sup>

For semicrystalline polymer, the impact strength varies with the change of temperature, and the impact strength at low temperature becomes more and more important because of the transition from ductile to brittle with decrease of temperature. The impact strength of crosslinked HDPE samples with different crosslink density are shown in Fig. 6(b). The amount of energy required to break the crosslinked HDPE varies widely with temperature and the content of BIPB. Compared with the un-crosslinked HDPE, the impact strength of crosslinked HDPE with 0.1% BIPB barely changes in the temperature of  $-60$  °C



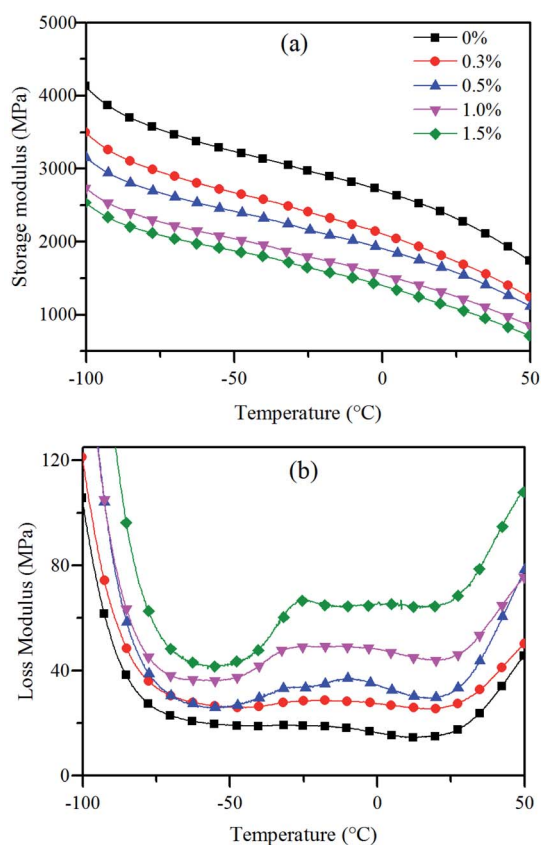


Fig. 7 Dynamic mechanical properties of the crosslinked HDPE: storage modulus (a) and loss modulus (b).

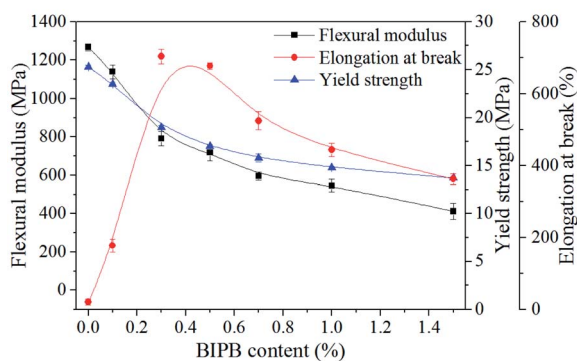


Fig. 8 Mechanical properties of crosslinked HDPE at 23 °C.

and 23 °C. For the crosslinked HDPE with high crosslink density, a dramatic change in the impact strength is observed when the temperature exceeds its brittle–ductile transition temperature (BDTT). The BDTT of the crosslinked HDPE decreases with increase in BIPB content.

### 3.6 Dynamic mechanical properties

Dynamic mechanical analysis (DMA) over wide temperature ranges gives detailed information of the chemical and physical structure of polymer which is related to its mechanical

properties. According to the literature, DMA of PE reveals three peaks, known at  $\alpha$ ,  $\beta$ ,  $\gamma$  transition, in which the  $\beta$  transition temperature is attributed to the amorphous phase. The  $\beta$  transition occurs between  $-30$  °C and  $10$  °C, and it is generally described that the  $\beta$  transition is due to the motion of branches in the amorphous matrix.<sup>43,44</sup> It has also been shown that  $\beta$  transition is the glass transition temperature which is related to transition of dynamic mechanical properties.<sup>45</sup>

The dynamic mechanical properties of the crosslinked HDPE were investigated. The results are displayed in Fig. 7. The storage modulus increases with decrease in temperature due to the decrease of free volume, and the storage modulus decreases with increase in BIPB content because of decrease in crystallinity. For the un-crosslinked polyethylene, the  $\beta$  transition is very little and hardly to be seen. With increase in BIPB content, the  $\beta$  transition increases significantly and the  $\beta$  transition peak becomes more and more evident.

In fact, with increase in BIPB content, more and more crosslinks are formed and the crosslink density of the crosslinked HDPE increases. The crystallinity, lamellar thickness and crystal size decrease. The content of amorphous phase increases, leading to increase in the intensity of  $\beta$  transition. With increase in BIPB content, the increase of  $\beta$  transition contributes to the increase of energy dissipation during impact tests, leading to increase of the impact strength at low temperature.

### 3.7 Mechanical properties

The mechanical properties of the crosslinked HDPE were also investigated and the results are shown in Fig. 8. The flexural modulus and the yield strength decrease with increase in BIPB content because of the decrease in crystallinity. The elongation at break increases with increase in BIPB content in the range of 0% and 0.7% because of the decrease in crystallinity and increase in ductility. The elongation at break decreases with further increase in BIPB content, and this is probably attributed to the suppression of mobility and orientation of the molecular chains during elongation.

## 4. Conclusions

HDPE is crosslinked with different content of peroxide (BIPB). It is found that, with increase in BIPB content, the elasticity, viscosity and gel content increase significantly, and the crystallinity, lamellar thickness, spherulitic size and crystal size decrease. The decrease of the lamellar thickness and crystal size increase the ductility. With decrease of crystallinity, the content of amorphous phase increases, leading to increase of the intensity of  $\beta$  transition and energy dissipation, and the brittle–ductile transition temperature decreases. The impact strength at low temperature increases significantly. With increase in the crosslinking density, the modulus and yield strength of the crosslinked HDPE decrease because of decrease in crystallinity, while the elongation at break exhibits an maximum with sharp increase at low BIPB content and then decrease gradually at higher BIPB content because of the competition between



## Paper

increase of toughness and decrease of mobility during orientation.

## Conflicts of interest

There are no conflicts to declare.

## Acknowledgements

The project was supported by the Beijing Municipal Science & Technology Commission (Z181100005218004).

## Notes and references

- G. L. Oliveira and M. F. Costa, *Mater. Sci. Eng., A*, 2010, **527**, 4593–4599.
- C. Jiao, Z. Wang, X. Liang and Y. Hu, *Polym. Test.*, 2005, **24**, 71–80.
- P. Kurian, K. E. George and D. J. Francis, *Eur. Polym. J.*, 1992, **28**, 113–116.
- Z. Bartczak, A. S. Argon, R. E. Cohen and M. Weinberg, *Polymer*, 1999, **40**, 2347–2365.
- Z. Bartczak, A. S. Argon, R. E. Cohen and M. Weinberg, *Polymer*, 1999, **40**, 2331–2346.
- S. C. Tjong and S. P. Bao, *Compos. Sci. Technol.*, 2007, **67**, 314–323.
- T. Liu, A. Huang, L.-H. Geng, X.-H. Lian, B.-Y. Chen, B. S. Hsiao, T.-R. Kuang and X.-F. Peng, *Compos. Sci. Technol.*, 2018, **167**, 301–312.
- L. Zhang, C. Li and R. Huang, *J. Polym. Sci., Part B: Polym. Phys.*, 2004, **42**, 1656–1662.
- Y. Wang, F. Lv, Y. Song, Y. Yang, Y. Cao, J. Wang, C. Li and W. Wang, *Polym. Test.*, 2020, **81**, 106280.
- M. Tanniru and R. D. K. Misra, *Mater. Sci. Eng., A*, 2005, **405**, 178–193.
- M. Tanniru, Q. Yuan and R. D. K. Misra, *Polymer*, 2006, **47**, 2133–2146.
- D. Bacci, A. B. Toaldo and M. Scaini, *J. Macromol. Sci., Part B: Phys.*, 2013, **52**, 1438–1452.
- H. A. Khonakdar, S. H. Jafari, U. Wagenknecht and D. Jehnichen, *Radiat. Phys. Chem.*, 2006, **75**, 78–86.
- H. A. Khonakdar, S. H. Jafari and R. Hässler, *J. Appl. Polym. Sci.*, 2007, **104**, 1654–1660.
- H. A. Khonakdar, S. H. Jafari, M. Taheri, U. Wagenknecht, D. Jehnichen and L. Häussler, *J. Appl. Polym. Sci.*, 2006, **100**, 3264–3271.
- J. Carlos Miguez Suarez and E. Biasotto Mano, *Polym. Test.*, 2000, **19**, 607–616.
- S. Yu, C. Park, S. M. Hong and C. M. Koo, *Thermochim. Acta*, 2014, **583**, 67–71.
- R. M. Gohil and P. J. Phillips, *Polymer*, 1986, **27**, 1696–1704.
- R. M. Gohil and P. J. Phillips, *Polymer*, 1986, **27**, 1687–1695.
- Y. H. Kao and P. J. Phillips, *Polymer*, 1986, **27**, 1669–1678.
- P. J. Phillips and Y. H. Kao, *Polymer*, 1986, **27**, 1679–1686.
- H. A. Khonakdar, J. Morshedean, M. Mehrabzadeh, U. Wagenknecht and S. H. Jafari, *Eur. Polym. J.*, 2003, **39**, 1729–1734.
- Y.-T. Shieh and H.-C. Chuang, *J. Appl. Polym. Sci.*, 2001, **81**, 1808–1816.
- A. G. Andreopoulos and E. M. Kampouris, *J. Appl. Polym. Sci.*, 1986, **31**, 1061–1068.
- A. Smedberg, T. Hjertberg and B. Gustafsson, *Polymer*, 2003, **44**, 3395–3405.
- A. Smedberg, T. Hjertberg and B. Gustafsson, *Polymer*, 1997, **38**, 4127–4138.
- H. A. Khonakdar, J. Morshedean, U. Wagenknecht and S. H. Jafari, *Polymer*, 2003, **44**, 4301–4309.
- R. Wang, D. Ren, X. Sun, W. Liang and K. Wang, *J. Appl. Polym. Sci.*, 2019, **136**, 47542.
- W. Cui, Y. Bian, H. Zeng, X. Zhang, Y. Zhang, X. Weng, S. Xin and Z. Jin, *J. Mech. Behav. Biomed. Mater.*, 2020, **104**, 103629.
- M. G. Andersson, M. Jarvid, A. Johansson, S. Gubanski, M. R. S. Foreman, C. Müller and M. R. Andersson, *Eur. Polym. J.*, 2015, **64**, 101–107.
- I. Carpentieri, V. Brunella, P. Bracco, M. C. Paganini, E. M. Brach del Prever, M. P. Luda, S. Bonomi and L. Costa, *Polym. Degrad. Stab.*, 2011, **96**, 624–629.
- X. Sun, H. Shen, B. Xie, W. Yang and M. Yang, *Polymer*, 2011, **52**, 564–570.
- F. R. Passador, A. C. Ruvolo-Filho and L. A. Pessan, *J. Appl. Polym. Sci.*, 2013, **130**, 1726–1735.
- E. Roumeli, K. M. Paraskevopoulos, D. Bikiaris and K. Chrissafis, *J. Mater. Sci.*, 2013, **48**, 6753–6761.
- W. Zhou and S. Zhu, *Macromolecules*, 1998, **31**, 4335–4341.
- T. Ikehara and T. Kataoka, *Sci. Rep.*, 2013, **3**, 1444.
- A. J. Lovinger, *Macromolecules*, 2020, **53**, 741–745.
- A. Toda, M. Okamura, K. Taguchi, M. Hikosaka and H. Kajioka, *Macromolecules*, 2008, **41**, 2484–2493.
- S. Sasaki, Y. Sakaki, A. Takahara and T. Kajiyama, *Polymer*, 2002, **43**, 3441–3446.
- J. A. Puértolas, F. J. Pascual and M. J. Martínez-Morlanes, *J. Mech. Behav. Biomed. Mater.*, 2014, **30**, 111–122.
- W. G. Perkins, *Polym. Eng. Sci.*, 1999, **39**, 2445–2460.
- S. J. A. Hocker, W. T. Kim, H. C. Schniepp and D. E. Kranbuehl, *Polymer*, 2018, **158**, 72–76.
- M. Sethi, N. K. Gupta and A. K. Srivastava, *J. Appl. Polym. Sci.*, 2002, **86**, 2429–2434.
- Y. P. Khanna, E. A. Turi, T. J. Taylor, V. V. Vickroy and R. F. Abbott, *Macromolecules*, 2002, **18**, 1302–1309.
- Y. P. Khanna, E. A. Turi, T. J. Taylor, V. V. Vickroy and R. F. Abbott, *Macromolecules*, 1985, **18**, 1302–1309.

